

BlobCtrl: A Unified and Flexible Framework for Element-level Image Generation and Editing

Yaowei Li¹ Lingen Li² Zhaoyang Zhang³ ‡ Xiaoyu Li³ Guangzhi Wang³ Hongxiang Li¹ Xiaodong Cun³
Ying Shan³ Yuexian Zou¹ *

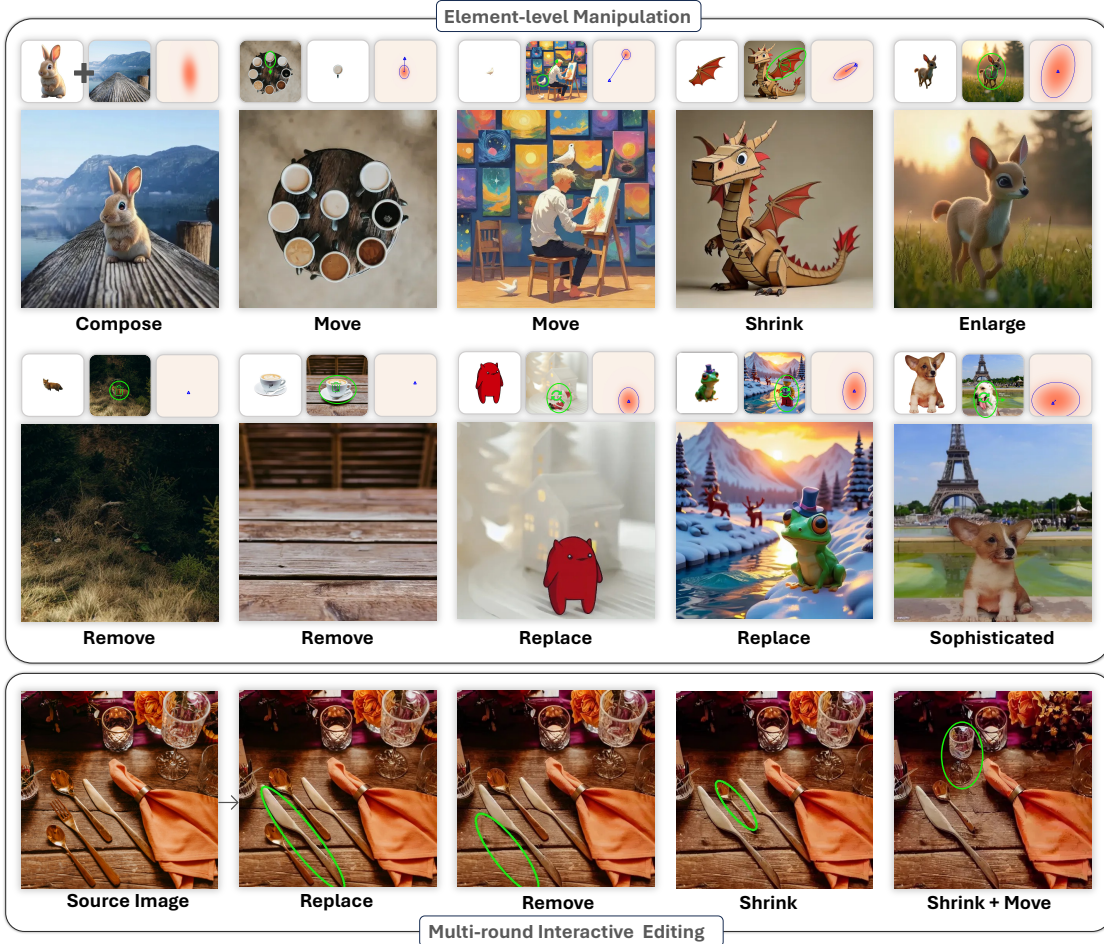


Figure 1: Our proposed *BlobCtrl* framework enables comprehensive element-level control over both visual appearance and spatial layout, facilitating diverse manipulation operations including compositional generation, spatial transformation, element removal, content replacement and arbitrary combinations thereof (top). Through an iterative refinement process, *BlobCtrl* allows precise and fine-grained editing capabilities to achieve desired visual outcomes (bottom).

Abstract

Element-level visual manipulation is essential in digital content creation, but current diffusion-

based methods lack the precision and flexibility of traditional tools. In this work, we introduce *BlobCtrl*, a framework that unifies element-level generation and editing using a probabilistic blob-based representation. By employing blobs as visual primitives, our approach effectively decouples and represents spatial location, semantic content, and identity information, enabling precise

¹Peking University ²The Chinese University of Hong Kong
³ARC Lab, Tencent PCG. ‡ Project lead: Zhaoyang Zhang
<zhaoyangzhang@link.cuhk.edu.hk>. * Corresponding author:
Yuexian Zou <zouyx@pku.edu.cn>.

element-level manipulation. Our key contributions include: 1) a dual-branch diffusion architecture with hierarchical feature fusion for seamless foreground-background integration; 2) a self-supervised training paradigm with tailored data augmentation and score functions; and 3) controllable dropout strategies to balance fidelity and diversity. To support further research, we introduce *BlobData* for large-scale training and *BlobBench* for systematic evaluation. Experiments show that *BlobCtrl* excels in various element-level manipulation tasks while maintaining computational efficiency, offering a practical solution for precise and flexible visual content creation. Project page: <https://liyaowei-stu.github.io/project/BlobCtrl/>.

1. Introduction

Element-level image manipulation has long been a goal in digital art, with tools like Adobe Photoshop(Adobe Inc., 1988–2023) enabling precise manipulation of visual elements. While recent AI models(Ramesh et al., 2022; Labs, 2023; Esser et al., 2024; Sheynin et al., 2024; Shi et al., 2024) excel in high-quality image synthesis, they often lack fine-grained control over individual elements—a key feature of traditional tools (Adobe Inc., 1988–2023; Serif Europe Ltd., 2015–2023). Advances like ControlNet(Zhang et al., 2023a) and IP-Adapter(Ye et al., 2023) have improved controllability but still do not support interactive, multi-round, element-based manipulation (e.g., composition, resizing, arrangement) crucial for creative workflows. Challenges include: 1) decoupling and representation of visual elements, 2) continuous layout control, 3) preserving appearance and identity, 4) maintaining visual harmony, and 5) scarcity of large-scale paired training data for end-to-end training.

Current efforts in element-level manipulation focus on two approaches: generation and editing, each facing obstacles. *Element-level generation*(Li et al., 2023; Ye et al., 2023; Nie et al., 2024; Chen et al., 2023; Xiong et al., 2024; Parmar et al., 2025) uses grounding tokens (e.g., bounding boxes, ellipses) for spatial control and identity tokens like CLIP(Radford et al., 2021) and DINO(Caron et al., 2021) for appearance maintenance. These methods struggle with continuous layout control due to the discrete nature of grounding tokens and the high compression of identity tokens, which hinders detailed appearance preservation. *Element-level editing* (Zhang et al., 2023b; Avrahami et al., 2023; Shi et al., 2023; Alzayer et al., 2024; Mu et al., 2025) employs optimization, segmentation, clustering, and drag-based methods for attribute control. These approaches often lack flexibility and struggle with visual harmony, frequently relying on video data that introduces complexities like cam-

era movements, degrading performance and generalization. Detailed discussions of related research works are provided in Section 5.

The essence of element-level visual modeling lies in the flexible decoupling and representation of location, semantics, and identity. *BlobCtrl* uses blobs as visual primitives to achieve this. Formally, a blob is a probabilistic two-dimensional Gaussian distribution(Carson et al., 1999), and geometrically, it appears as an ellipse(Nie et al., 2024). Blob parameters precisely specify position, size, and orientation, while Gaussian smoothness ensures harmonious and continuous layout control. For visual identity, we use differentiable blob splatting(Epstein et al., 2022) combined with variational autoencoder (VAE) features(Kingma, 2013) to preserve appearance.

Building on the probabilistic blob representation, we introduce a dual-branch diffusion model: one branch for foreground elements and another for background elements. A self-supervised training paradigm enhances generalization and efficiency, with specific strategies improving *BlobCtrl*’s robustness. To preserve foreground identities, we propose random data augmentation and an ID retention score function. Additionally, random dropout in the dual-branch structure allows flexible balancing of appearance fidelity and creative diversity during inference. These design choices make *BlobCtrl* an efficient, flexible solution for element-level generation and editing.

To scale up our method and ensure comprehensive evaluation, we introduce a new training dataset, *BlobData*, and a benchmark, *BlobBench*. Extensive quantitative and qualitative results demonstrate *BlobCtrl*’s effectiveness in element-level generation (combining multiple subjects) and editing (moving, resizing, adding, deleting, and replacing elements).

In a nutshell, our main contributions include:

- We propose *BlobCtrl*, a novel unified framework that first enables precise and flexible manipulation over visual elements through element-level generation and editing, while effectively preserving their intrinsic characteristics.
- We design an innovative dual-branch architecture with meticulously crafted training paradigms and strategies, achieving an optimal balance between maintaining appearance fidelity and enabling creative diversity in visual manipulation.
- We introduce *BlobData*, a comprehensive large-scale dataset specifically curated for training element-level visual models, alongside *BlobBench*, a rigorous evaluation benchmark for assessing element-level generation and editing capabilities.
- Through extensive experimentation, we demonstrate that *BlobCtrl* achieves superior performance compared to existing methods in both element-level generation and editing.

ing tasks, while maintaining computational efficiency and practical applicability.

2. Blob-Based Element-level Representation

Why is the blob an effective element-level representation? As a grounding token, a blob precisely represents an object’s position, size, and orientation. As a Gaussian distribution, it offers more flexible and harmonious element-level expression than segmentation masks, which have strong shape constraints. In this section, we define the blob and explain its role as an element-level visual representation.

2.1. Blob Formula

Fig. 2 visualizes a blob. Geometrically, a blob can be considered as an ellipse, parameterized by $e_r = [C_x, C_y, a, b, \theta]$, where C_x and C_y denote the coordinates of the ellipse’s center, a and b are the lengths of the minor and major axes, respectively, and $\theta \in [0, \pi]$ is the orientation angle of the ellipse. Statistically, a blob is modeled as a two-dimensional Gaussian distribution, parameterized by $\mu = [\mu_x, \mu_y]$ and $\Sigma = \begin{bmatrix} \sigma_{xx} & \sigma_{xy} \\ \sigma_{yx} & \sigma_{yy} \end{bmatrix}$, where μ_x and μ_y are the means of the Gaussian distribution, $[\sigma_{xx}, \sigma_{yy}]$ are the variances corresponding to the x and y directions, respectively, and $[\sigma_{xy}, \sigma_{yx}]$ are the covariances, indicating the correlation between x and y .

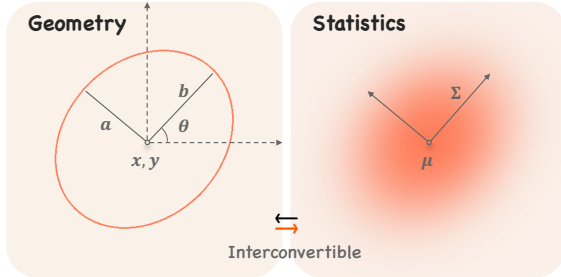


Figure 2: **Blob Formula.** A blob can be represented in two equivalent forms: geometrically as an ellipse parameterized by center coordinates (C_x, C_y) , axes lengths (a, b) , and orientation θ ; and statistically as a 2D Gaussian distribution characterized by mean μ and covariance matrix Σ . The two forms are exactly equivalent and interchangeable.

2.2. Blob Opacity

Notably, the blob represented as a Gaussian enables the calculation of opacity across spatial dimensions, leading to the concepts of blob splatting and blob composition. These concepts are crucial for achieving smooth rendering and seamless integration of visual elements in graphics.

In particular, the squared Mahalanobis distance (Maha-

lanobis, 1936) to the blob center is first computed:

$$d_M(\mathbf{x}_{\text{grid}}, \mathbf{Q}) = (\mathbf{x}_{\text{grid}} - \mu)^T \Sigma^{-1} (\mathbf{x}_{\text{grid}} - \mu), \quad (1)$$

where $\mathbf{x}_{\text{grid}} \in \left\{ \left(\frac{w}{W}, \frac{h}{H} \right) \right\}_{w=1, h=1}^{W, H}$ is a point on a two-dimensional grid map, and \mathbf{Q} represents the 2D Gaussian distribution of the blob, characterized by its mean μ and covariance matrix Σ . The distance $d_M \in \mathbb{R}^{H, W}$ quantifies how far the point \mathbf{x}_{grid} is from the center μ while taking into account the shape of the distribution defined by Σ . Then, the blob opacity can be calculated based on this distance:

$$O(\mathbf{x}_{\text{grid}}) = \text{sigmoid}(-d_M), \quad (2)$$

which maps the distance d_M to a value between 0 and 1, effectively representing the opacity of the blob at the point \mathbf{x}_{grid} . This ensures that points closer to the center of the blob have higher opacity, while those further away are more transparent, ensuring a smooth and continuous transition.

2.3. Blob Composition and Splatting

Blob composition implies the process of integrating multiple blobs through depth-aware alpha compositing (Porter & Duff, 1984; Nitzberg & Mumford, 1990), which effectively addresses occlusion and models inter-object relationships. Mathematically, blob composition is formulated as follows:

$$O_c^i(\mathbf{x}_{\text{grid}}) = O_i(\mathbf{x}_{\text{grid}}) \prod_{j=i+1}^m (1 - O_j(\mathbf{x}_{\text{grid}})), \quad (3)$$

where m is the total number of blobs to be composed, $O_c^i(\mathbf{x}_{\text{grid}}) \in \mathbb{R}^{h, w}$ represents the composed opacity of the i -th blob across spatial dimensions, and the product term accounts for the occlusion effects of subsequent blobs in the sequence. In our *BlobCtrl*, we compose the foreground and background element to obtain the foreground opacity O_{fg} and background opacity O_{bg} , which serve as an element-level layout representation.

Blob splatting (Epstein et al., 2022) refers to the ability to project m features $\mathbf{f}^i \in \mathbb{R}^{1 \times d}$ into a two-dimensional space via m blob, creating spatially-aware features $\mathbf{F} \in \mathbb{R}^{h \times w \times d}$. Formally, blob splatting is expressed as follows:

$$\mathbf{F} = g_{\text{splatting}}(\mathbf{f}, O_c) = \sum_{i=0}^m O_c^i \cdot \mathbf{f}^i, \quad (4)$$

where \cdot denotes element-wise multiplication with broadcasting. In our *BlobCtrl*, we first use DINO V2 (Oquab et al., 2023) to encode the visual semantics of the foreground element. The semantic features \mathbf{f}_{fg} are then splatted with the foreground opacity O_{fg} , resulting in spatially-aware, element-level visual semantic feature \mathbf{F}_{fg} .

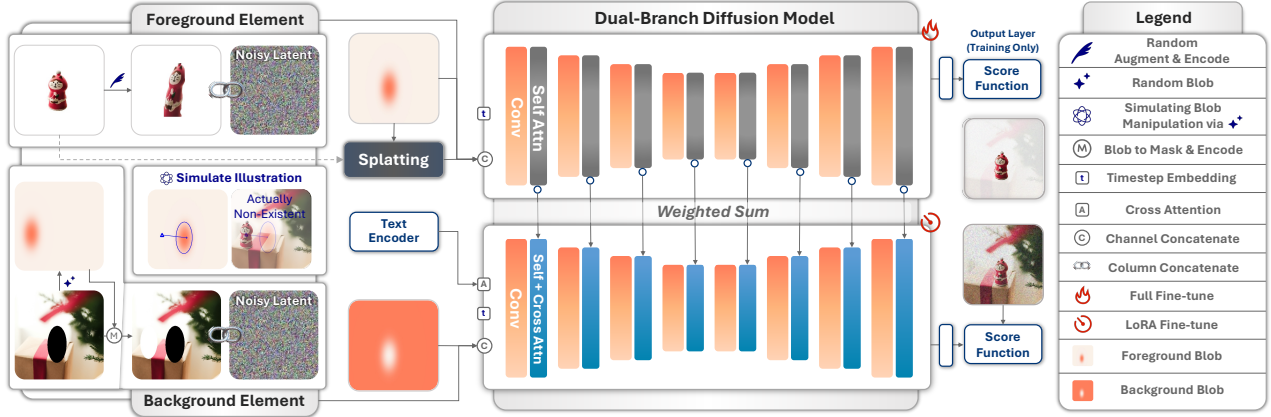


Figure 3: **Overview of BlobCtrl.** Our framework consists of: (1) A dual-branch architecture with a foreground branch for element identity encoding and a background branch for scene context preservation and harmonization. Both branches use concatenated inputs of noisy latents and reference conditions (Sec. 3.1). (2) A self-supervised training paradigm for element-level manipulation through stochastic position generation and target reconstruction optimization. Through feature fusion between branches, our framework achieves precise control over elements while maintaining visual coherence.

3. Self-supervised Paradigm for BlobCtrl

As discussed in Sec. 2, blob-based representation offers continuous spatial control for flexible manipulation, seamless composition for harmonious integration, and spatial-aware splatting for visual semantics. Leveraging these advantages, we introduce a self-supervised training paradigm to develop a robust and versatile model for element-level visual generation and editing.

3.1. Model Architecture

Based on the blob representation, we propose a dual-branch diffusion model to handle foreground and background elements separately. As shown in Fig. 3, our model mainly consists of two key components:

Foreground Branch. The foreground branch is designed to preserve the identity and appearance of foreground elements while enabling flexible layout control. As shown in Fig 3, we concatenate the noisy latent $z_t \in \mathbb{R}^{c,h,w}$ with reference foreground conditions $c_{fg} \in \mathbb{R}^{(c+1+d),h,w}$ along the column dimension as input to the foreground branch. This column-wise concatenation strategy improves the model’s in-context learning capabilities, allowing it to more effectively grasp and retain the characteristics of elements. The reference foreground conditions c_{fg} are constructed by concatenating three key components along the channel dimension: (1) the opacity map O_{fg} for layout information, (2) spatially-aware semantic features F_{fg} for identity preservation, and (3) VAE latent z_{fg} for appearance encoding. To ensure dimensional compatibility for the column-wise concatenation between z_t and c_{fg} , we additionally concatenate O_{fg} and F_{fg} along the channel dimension of z_t . The input construction process for the foreground branch can be

formally expressed as:

$$\text{input}_{fg} = [c_{fg}, [z_t, O_{fg}, F_{fg}; \text{axis} = 0]; \text{axis} = 2], \quad (5)$$

$$c_{fg} = [z_{fg}, O_{fg}, F_{fg}; \text{axis} = 0] \in \mathbb{R}^{(c+1+d),h,w}, \quad (6)$$

where $[\text{axis} = 0]$ and $[\text{axis} = 2]$ represent concatenation along the channel and column, respectively.

To process element-level foreground input, we use a modified pre-trained diffusion backbone with cross-attention layers removed. This approach serves two purposes: the pre-trained weights offer a strong generative prior for effective foreground feature processing, and removing cross-attention layers ensures the model focuses solely on visual content without broader contextual influences.

Background Branch. The background branch serves as a diffusion backbone aims to preserve the original background while harmoniously integrating foreground elements into the scene. Similarly, we concatenate the noisy latent z_t with reference background conditions c_{bg} along the column dimension as input, as shown below:

$$\text{input}_{bg} = [c_{bg}, [z_t, O_{bg}; \text{axis} = 0]; \text{axis} = 2], \quad (7)$$

$$c_{bg} = [z_{bg}, O_{bg}; \text{axis} = 0] \in \mathbb{R}^{(c+1),h,w}, \quad (8)$$

where background branch lacks spatial-aware semantic features, as it tends to preserve information completely.

In element-level editing, the background is the masked image where both the original and target regions of the foreground element are masked out. For instance, when moving a bird, the background has masks at both the bird’s initial and destination positions.

The background branch uses a complete diffusion backbone with cross-attention layers. To seamlessly integrate foreground and background elements, we employ hierarchical

feature fusion, progressively injecting foreground features at multiple resolution levels in the background branch. We also use zero-initialization (Zhang et al., 2023a) \mathcal{Z} for stable training. Feature fusion for the i -th block is formulated as:

$$\epsilon_{\theta}^i(z_t, t, C) = \epsilon_{\theta}^i(z_t, t, C') + \omega \cdot \mathcal{Z}(\epsilon_{\theta}^i(z_t, t, C')), \quad (9)$$

where C and C' is the input conditions for the background and the foreground branch respectively, and ω is the weight for feature fusion.

3.2. Self-supervised Training

While paired data of objects at different positions would be ideal for training, such data is scarce. Previous methods (Chen et al., 2023; Alzayer et al., 2024) rely on video data, but this introduces unwanted complexities that degrade model performance.

Instead, we propose a self-supervised training strategy, employing the idea that any image can be seen as the target result of an element manipulation process. For each training image, we identify the target element’s position and randomly generate a blob at a different location to simulate the source position. This mimics the manipulation process, as shown in Fig. 3, where a toy appears to move from a random left position to its actual right position. We optimize our model using a noise-prediction score function during training:

$$\mathcal{L} = \mathbb{E}_{z_0, C, C', \epsilon \sim \mathcal{N}(0, I)} [\|\epsilon - \epsilon_{\theta}(z_t, t, C, C')\|_2^2], \quad (10)$$

where z_0 is the latent of the source image and $z_t = \sqrt{\alpha_t}x_0 + \sqrt{1 - \alpha_t}\epsilon$ is the noisy latent at time step t . This score function drives the model to fill foreground elements at the target layout, inpaint background elements at the original foreground position, and ensure harmonious integration of the entire scene.

3.3. ID Preservation and Scene Harmonization

Random Data Augmentation. To prevent the model from defaulting to a simple copy-and-paste solution, we employ extensive data augmentation on foreground elements during training. This includes random transformations such as color jittering, scaling, rotation, erasing, and perspective changes. These augmentations serve two main purposes: they compel the model to harmoniously place foreground elements based on specified layouts and appearances, and the random erasing fosters robust inpainting capabilities for incomplete elements. This approach ensures the model learns to generate and manipulate elements flexibly and contextually, maintaining visual coherence with the background.

Identity Preservation Score Function. To effectively decouple the foreground and background branches—ensuring the foreground branch injects element-level information while the background branch integrates these elements—we

propose an identity preservation score function. During training, we retain the diffusion model’s output layer in the foreground branch (discarded during inference) and apply a score function that operates only within the foreground element region.

$$\mathcal{L}_{\text{id}} = \mathbb{E}_{z_0, C', \epsilon \sim \mathcal{N}(0, I)} [M_{\text{fg}} \cdot \|\epsilon - \epsilon_{\theta}(z_t, t, C')\|_2^2], \quad (11)$$

where M_{fg} is the foreground mask that indicates the foreground element region. This helps ensure accurate preservation of foreground element appearance while allowing flexibility in background integration. During training, the overall optimization objective is:

$$\mathcal{L}_{\text{total}} = \mathcal{L} + \lambda_{\text{id}} \mathcal{L}_{\text{id}}, \quad (12)$$

where λ_{id} is a hyperparameter that controls the weight of identity preservation. We gradually decay λ_{id} from 1.0 to 0.6 during training, which encourages the model to focus more on scene harmonization in later training stages while still maintaining reasonable identity preservation.

3.4. Controllable Fidelity-Diversity Trade-off

To achieve flexible control between appearance fidelity and creative diversity, we implement random dropout strategies during training. First, we randomly drop the weights of the foreground branch, allowing the model to adjust between freely generating foreground elements based on global textual information and strictly preserving given foreground identities. Second, we randomly drop both the semantic features to be splatted and the VAE features of foreground elements, enabling flexible control over the balance between semantics and appearance. Specifically, we apply:

$$\begin{aligned} \omega' &= \omega \cdot \mathbb{I}(\xi_1 < p_{\omega}) \\ \mathbf{F}'_{\text{fg}} &= \mathbf{F}_{\text{fg}} \cdot \mathbb{I}(\xi_2 < p_{\text{feat}}) \\ \mathbf{z}'_{\text{fg}} &= \mathbf{z}_{\text{fg}} \cdot \mathbb{I}(\xi_3 < p_{\text{vae}}) \end{aligned} \quad (13)$$

where \mathbb{I} is indicator function, and $\xi_1, \xi_2, \xi_3 \sim \mathcal{U}(0, 1)$ are uniform random variables, $p_{\omega}, p_{\text{feat}}, p_{\text{vae}}$ are the dropout probabilities for branch weights, semantic features, and VAE features respectively.

4. Experiments

4.1. Datasets, Benchmark and Metrics

BlobData Curation. To train *BlobCtrl*, we construct *BlobData* (1.86M samples) sourced from BrushData, containing images, segmentation masks, fitted ellipse parameters (with derived 2D Gaussians), and descriptive texts. The dataset curation process involves: (1) Filtering source images to retain those with shorter sides over 480 pixels and valid instance segmentation masks. (2) Applying mask filtering criteria to preserve masks with area ratios between 0.01 and 0.9 of the total image area and excluding those at image

Method	Compose			Move			Resize			Replace			Remove	
	CLIP-I \uparrow	DINO \uparrow	MSE \downarrow	CLIP-I \uparrow	DINO \uparrow	MSE \downarrow	CLIP-I \uparrow	DINO \uparrow	MSE \downarrow	CLIP-I \uparrow	DINO \uparrow	MSE \downarrow	CLIP-I* \downarrow	DINO* \downarrow
Anydoor (Chen et al., 2023)	86.7	81.2	6.7	85.4	81.7	6.8	83.3	83.7	9.6	81.7	80.2	9.7	39.5	13.6
GliGen (Li et al., 2023)	70.7	57.8	6.9	71.2	62.4	7.1	78.2	69.4	9.7	68.4	60.6	9.6	40.2	15.3
MagicFix (Alzayer et al., 2024)	80.5	78.6	6.9	84.6	82.4	6.7	83.7	85.2	9.0	84.2	80.1	9.4	43.6	23.1
<i>BlobCtrl</i> (Ours)	88.3	86.9	6.4	88.9	87.8	6.3	86.5	89.1	8.9	86.2	86.0	9.0	35.3	8.6

Table 1: Quantitative comparison of identity preservation and grounding accuracy across various element-level manipulations. We evaluate using CLIP-I and DINO scores for identity preservation, and MSE for grounding accuracy. For removal operations, lower CLIP-I* and DINO* scores (\downarrow) are desired as they indicate more complete removal of target elements. Our method consistently outperforms existing approaches across all operations.

Method	PSNR \uparrow	SSIM \uparrow	LPIPS \downarrow	FID \downarrow
Anydoor (Chen et al., 2023)	32.0631	0.7424	0.2394	145.2546
GliGen (Li et al., 2023)	27.923	0.2414	0.6963	307.8219
MagicFix (Chen et al., 2023)	30.3958	0.7415	0.2277	194.0154
<i>BlobCtrl</i> (Ours)	32.1571	0.7507	0.2196	102.8094

Table 2: Comparison of image generation quality using standard metrics. Our method achieves superior performance across all metrics, demonstrating better generation quality and fewer artifacts.

boundaries. (3) For the filtered masks, fitting ellipse parameters¹ and derive 2D Gaussian distributions. (4) Removing invalid samples, particularly those with covariance values below $1e-5$. (5) Generating detailed image descriptions with InternVL-2.5 (Chen et al., 2024).

BlobBench Curation. Existing evaluation benchmarks like DreamBooth(Ruiz et al., 2023), COCOE(Yang et al., 2023), COCO Val(Lin et al., 2014), and CreatiLayout(Zhang et al., 2024a) assess either grounding capability or identity preservation, but not both simultaneously. They also lack coverage of the full range of element-level manipulations, such as composition, movement, resizing, deletion, and replacement. To address these gaps, we introduce *BlobBench*, a comprehensive benchmark with 100 curated images, evenly distributed across different element-level operations. Each image is annotated with ellipse parameters, a foreground mask, and detailed text descriptions by experts. *BlobBench* includes both real-world and AI-generated images across diverse scenarios, such as indoor and outdoor scenes, animals, and landscapes, ensuring a fair and effective evaluation.

Evaluation Metrics. We evaluate *BlobCtrl* using both objective metrics and human assessment, including objective evaluation (identity preservation, grounding accuracy, generation quality and harmonization) and subjective evaluation. Please refer to the Appendix A for details about these metrics.

¹https://docs.opencv.org/4.x/de/d62/tutorial_bounding_rotated_ellipses.html

4.2. Implementation Details.

Training Details. *BlobCtrl* is built upon Stable Diffusion v1.5 (Rombach et al., 2022). During training, all images and annotations are resized to 512×512 pixels. We initialize both foreground and background branches with pretrained UNet weights. The foreground branch undergoes full fine-tuning with cross-attention layers removed, while the background branch is fine-tuned using LoRA (Hu et al., 2021) with rank=64. We employ the Adam optimizer (Kingma & Ba, 2014) with a learning rate of $1e-5$ and weight decay of 0.01. The model is trained on our curated *BlobData* dataset comprising 1.86M samples for 7 days using 24 NVIDIA V100 GPUs with a batch size of 192. For controllable fidelity-diversity trade-off, we set dropout probabilities p_w, p_{feat}, p_{vae} to 0.1. The weight of identity preservation loss λ_{id} is gradually decayed from 1.0 to 0.6 during training. Additionally, to enable classifier-free guidance during inference, we set the caption dropout probability to 0.1.

Evaluation Details. We evaluate *BlobCtrl* against three state-of-the-art methods on the *BlobBench* benchmark: GliGen(Li et al., 2023), a bounding box-based text-to-image model; Anydoor(Chen et al., 2023), a segmentation mask-based image-to-image model; and Magic Fixup (Chen et al., 2023), which specializes in harmonizing transformed regions. To systematically assess five fundamental element-level operations (composition, movement, resizing, replacement, and removal), we adapt the baselines with specific workflows. For Anydoor, we create a clean background by teleporting background to foreground regions, then edit by teleporting foreground objects to target locations. For GliGen, we use *BlobCtrl* to remove elements for a clean background, then apply bounding box constraints with text and image conditions. For Magic Fixup, we warp foreground elements using rigid transformations from editing operations, followed by scene harmonization.

4.3. Quantitative Evaluation

Comparison to State-of-the-Art Methods. As shown in Tab. 1 and Tab. 2, *BlobCtrl* demonstrates consistent and significant improvements over existing methods across all evaluation metrics:

- **Identity Preservation:** For tasks requiring identity preser-

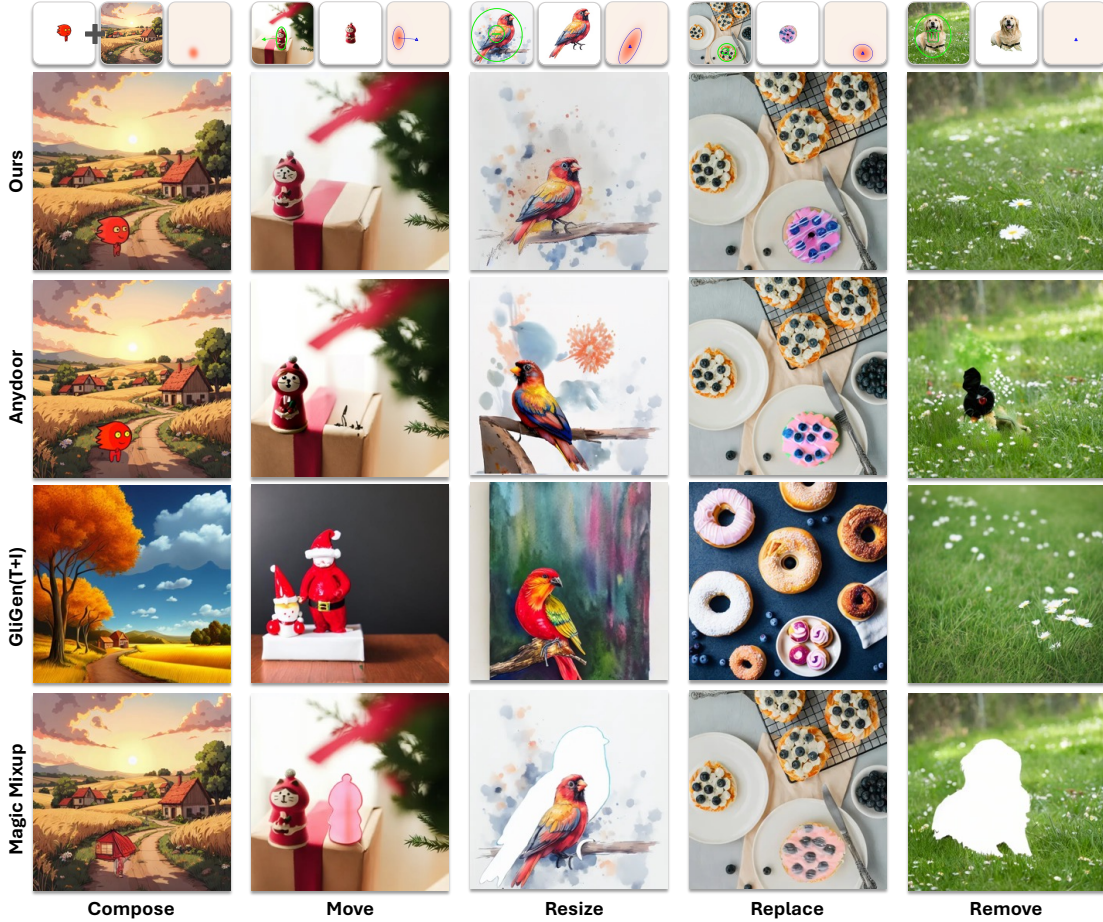


Figure 4: **Visual comparison of element-level manipulation capabilities across different methods.** We evaluate five fundamental operations: composition, movement, resizing, replacement and removal. Anydoor (Chen et al., 2023) struggles with precise identity preservation, GliGen (Li et al., 2023) fails to maintain any identity information, and Magic Mixup (Chen et al., 2023) produces results with poor visual harmonization. In contrast, *BlobCtrl* achieves superior results across all operations while maintaining both identity preservation and visual harmony. We recommend zooming in to examine the source images and element-level manipulation instructions in detail.

vation (composition, movement, resizing, replacement), *BlobCtrl* achieves substantially higher average CLIP-I (87.48 vs. 84.28) and DINO (87.45 vs. 81.70) scores compared to the best baseline. For removal tasks, our method shows lower identity scores (average of CLIP-I* and DINO* scores) (21.95 vs. 26.55), indicating more thorough element elimination.

- **Layout Control:** *BlobCtrl* exhibits superior spatial control accuracy, reducing layout MSE by 8.11% relative to the previous best method. This validates the effectiveness of our probabilistic blob representation for precise element manipulation.
- **Generation Quality:** Our method sets new state-of-the-art performance benchmarks across standard quality metrics: FID 102.8094, LPIPS 0.2196, PSNR 32.1571, and SSIM 0.7507. These results demonstrate *BlobCtrl*'s ability to generate high-fidelity outputs while maintaining global visual coherence.

We attribute these substantial improvements to two key innovations: (1) the probabilistic blob representation that enables precise control over element attributes, and (2) our self-supervised training paradigm that effectively decouples and recombines visual elements' identity, semantics and layout information, while eliminating performance degradation caused by unnecessary camera movements and other video-specific artifacts that plague previous methods.

Human Evaluation. The subjective evaluation results reported in Tab. 3 demonstrate the superior performance of *BlobCtrl* across all assessment criteria. Quantitatively, our method establishes new state-of-the-art performance with significant margins over the previous best approach: an 87.2% preference rate in appearance fidelity compared to 82.5% for the previous best method, an 86.5% preference rate in layout accuracy versus 81.7%, and an 82.1% preference rate in visual harmony compared to 80.3%. These substantial improvements in human evaluation metrics in-

indicate that *BlobCtrl* produces results that are more visually appealing and natural to human observers, making it better suited for real-world applications.

Method	Fidelity \uparrow	Layout \uparrow	Harmony \uparrow
Anydoor (Chen et al., 2023)	82.5%	81.7%	78.1%
GliGen (Li et al., 2023)	51.2%	68.1%	80.3%
MagicFix (Chen et al., 2023)	70.2%	73.1%	49.4%
<i>BlobCtrl</i> (Ours)	87.2%	86.5%	82.1%

Table 3: **Human evaluation results comparing our method with baselines.** Our method achieves consistently higher human preference scores across all metrics, demonstrating superior perceptual quality.

4.4. Qualitative Evaluation

Fig. 4 presents qualitative comparisons between *BlobCtrl* and state-of-the-art methods across various element-level manipulation scenarios. The results demonstrate several key advantages of our approach:

- Anydoor (Chen et al., 2023) struggles with accurate identity preservation during element manipulation and shows limitations in element-level removal, often leaving artifacts or incomplete modifications.
- While GliGen (Li et al., 2023) provides layout control capabilities, it fails to effectively preserve the visual appearance and identity of manipulated elements, resulting in inconsistent outputs.
- Magic Mixup (Alzayer et al., 2024) exhibits insufficient harmonization abilities, leading to visual inconsistencies between modified elements and their surroundings.

In contrast, *BlobCtrl* demonstrates superior performance across all aspects - better generalization to diverse scenarios, more accurate identity preservation, and precise layout control while maintaining visual coherence.

4.5. Ablation Studies

Analysis of Controllability and Flexibility As shown in Fig. 5, *BlobCtrl* achieves flexible control over the trade-off between identity preservation and diversity by adjusting the control timestep interval and control strength ω of the dual-branch fusion. When using only the background branch with text prompts, both identity preservation and layout accuracy suffer. Best results come from combining spatial-aware semantic features s_{fg} and VAE features z_{vae} .

Ablation of Identity Preservation Score Function. We conduct an ablation study to analyze the effectiveness of our Identity Preservation Score Function. As shown in Fig. 6, under the same training steps, the model with Identity Preservation Score Function achieves significantly lower noise prediction loss (0.0235) compared to the model without it (0.0399), demonstrating faster convergence. To better understand how this score function affects the generation process, we visualize the denoising results using the pre-

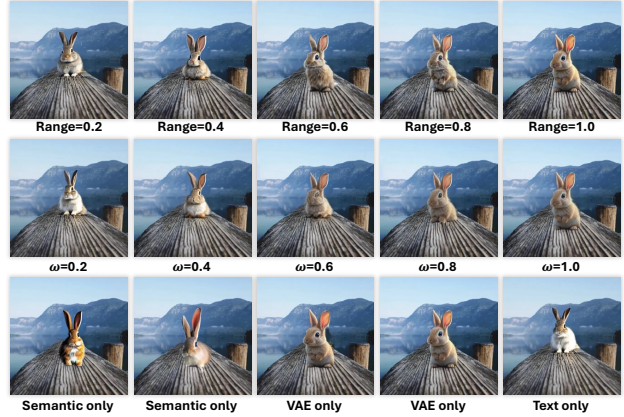


Figure 5: **Flexible Control.** Our dual-branch fusion mechanism enables flexible control over the trade-off between diversity and appearance preservation by adjusting the control timestep interval and fusion strength ω . Additionally, the feature dropout mechanisms provide more flexible interfaces for controlling the generation process.

dicted noise from the foreground branch. The visualization reveals that the foreground branch effectively focuses on generating foreground content when guided by the Identity Preservation Score Function, validating our design choice of decoupling foreground and background element generation through this mechanism.



Figure 6: **Ablation of Identity Preservation Score Function.** Training loss and denoising visualization for scaling a deer, demonstrating how Identity Preservation Score Function enables faster convergence and effective foreground-background decoupling during element-level manipulation.

5. Related Work

Element-level Generation. Contemporary element-level generation approaches can be categorized into two main paradigms: grounding-based and subject-driven methods. *Grounding-based* approaches, exemplified by GliGen and BlobGen (Li et al., 2023; Nie et al., 2024), employ bounding boxes and ellipses to achieve spatial control. However, these methods lack robust identity control mechanisms, resulting in significant content variations across different random initializations. While VisualComposer (Parmar et al., 2025) advances the field by incorporating multi-granular encoders for identity feature extraction, it struggles with precise layout control. Although Anydoor (Chen et al., 2023) and GroundingBooth (Xiong et al., 2024) demonstrate promising results

in controlling both identity and layout, their heavy reliance on multi-view and video training data constrains their practical applicability and generalization capabilities. In the realm of *subject-driven* approaches, existing methods face significant limitations - they either demand computationally expensive test-time optimization (Gal et al., 2022; Ruiz et al., 2023; Gal et al.; Kumari et al., 2023) or depend extensively on multi-view datasets (Arar et al., 2023; Wei et al., 2023; Li et al., 2024a; Zhang et al., 2024b), which impedes their out-of-distribution generalization and spatial control capabilities. In contrast, our *BlobCtrl* presents an elegant solution by seamlessly integrating layout, semantic, and identity information through probabilistic blob representations and self-supervised training, thereby achieving flexible control over both appearance fidelity and creative diversity.

Element-level Editing. Traditional image editing methods (Hertz et al., 2023; Brooks et al., 2023; Huang et al., 2024; Cao et al., 2023; Li et al., 2024b; Shi et al., 2024) rely on text prompts to introduce editing information, while element-level editing methods focus on manipulating visual elements through operations like moving, resizing, replacing and removal. Continuous Layout Editing (Zhang et al., 2023b) decouples layout and appearance through test-time optimization but suffers from high computational costs. Magic Fixup (Alzayer et al., 2024) introduces a two-stage pipeline consisting of transformation and harmonization steps, but relies on video data for training which can lead to degraded performance. Editable-element (Mu et al., 2025) proposes an element-level VAE approach but shows limited generalization ability due to its heavy dependence on large-scale paired training data. In contrast, our approach enables flexible element-level editing through self-supervised training, eliminating the need for explicitly paired editing data.

6. Discussion

Conclusion. This work introduces *BlobCtrl*, a unified framework that integrates element-level generation and editing using a probabilistic blob-based representation. Blobs serve as visual primitives to encode spatial layout, semantics, and identity, allowing precise element manipulation. The dual-branch architecture with self-supervised training preserves foreground identities and maintains background harmony. Random data augmentation and dropout strategies offer flexible control between appearance fidelity and creative diversity. Extensive experiments on *BlobBench* demonstrate that *BlobCtrl* achieves state-of-the-art performance in element-level manipulation tasks.

Limitations and Future Work. While *BlobCtrl* demonstrates strong capabilities in element-level manipulation, it currently only supports iterative single-element operations

in a single model forward pass. Fortunately, observersur blob-based representation inherently supports depth-aware composition, opening promising directions for future work.

Impact Statement

Our work on element-level manipulation presents both opportunities and risks. While it enables more precise and flexible creative tools, there are potential concerns about misuse for creating misleading or harmful content. We advocate for responsible development and deployment of such technologies, with clear guidelines for ethical use and transparency about AI-generated content.

References

- Adobe Inc. Adobe photoshop, 1988–2023. URL <https://www.adobe.com/products/photoshop.html>. Version 2023.
- Alzayer, H., Xia, Z., Zhang, X., Shechtman, E., Huang, J.-B., and Gharbi, M. Magic fixup: Streamlining photo editing by watching dynamic videos. *arXiv preprint arXiv:2403.13044*, 2024.
- Arar, M., Gal, R., Atzmon, Y., Chechik, G., Cohen-Or, D., Shamir, A., and H. Bermano, A. Domain-agnostic tuning-encoder for fast personalization of text-to-image models. In *SIGGRAPH Asia 2023 Conference Papers*, pp. 1–10, 2023.
- Avrahami, O., Aberman, K., Fried, O., Cohen-Or, D., and Lischinski, D. Break-a-scene: Extracting multiple concepts from a single image. In *SIGGRAPH Asia 2023 Conference Papers*, pp. 1–12, 2023.
- Brooks, T., Holynski, A., and Efros, A. A. Instructpix2pix: Learning to follow image editing instructions. In *Proceedings of the IEEE/CVF Conference on Computer Vision and Pattern Recognition*, pp. 18392–18402, 2023.
- Cao, M., Wang, X., Qi, Z., Shan, Y., Qie, X., and Zheng, Y. Masactrl: Tuning-free mutual self-attention control for consistent image synthesis and editing. In *Proceedings of the IEEE/CVF International Conference on Computer Vision (ICCV)*, pp. 22560–22570, October 2023.
- Caron, M., Touvron, H., Misra, I., Jégou, H., Mairal, J., Bojanowski, P., and Joulin, A. Emerging properties in self-supervised vision transformers. In *Proceedings of the IEEE/CVF international conference on computer vision*, pp. 9650–9660, 2021.
- Carson, C., Thomas, M., Belongie, S., Hellerstein, J. M., and Malik, J. Blobworld: A system for region-based image indexing and retrieval. In *Visual Information and Information Systems: Third International Conference*,

- VISUAL'99 Amsterdam, The Netherlands, June 2–4, 1999 Proceedings 3*, pp. 509–517. Springer, 1999.
- Chen, X., Huang, L., Liu, Y., Shen, Y., Zhao, D., and Zhao, H. Anydoor: Zero-shot object-level image customization. *arXiv preprint*, 2023.
- Chen, Z., Wang, W., Cao, Y., Liu, Y., Gao, Z., Cui, E., Zhu, J., Ye, S., Tian, H., Liu, Z., et al. Expanding performance boundaries of open-source multimodal models with model, data, and test-time scaling. *arXiv preprint arXiv:2412.05271*, 2024.
- Epstein, D., Park, T., Zhang, R., Shechtman, E., and Efros, A. A. Blobgan: Spatially disentangled scene representations. In *European Conference on Computer Vision*, pp. 616–635. Springer, 2022.
- Esser, P., Kulal, S., Blattmann, A., Entezari, R., Müller, J., Saini, H., Levi, Y., Lorenz, D., Sauer, A., Boesel, F., et al. Scaling rectified flow transformers for high-resolution image synthesis. In *Forty-first International Conference on Machine Learning*, 2024.
- Gal, R., Alaluf, Y., Atzmon, Y., Patashnik, O., Bermano, A. H., Chechik, G., and Cohen-or, D. An image is worth one word: Personalizing text-to-image generation using textual inversion. In *The Eleventh International Conference on Learning Representations*.
- Gal, R., Alaluf, Y., Atzmon, Y., Patashnik, O., Bermano, A. H., Chechik, G., and Cohen-Or, D. An image is worth one word: Personalizing text-to-image generation using textual inversion. *arXiv preprint arXiv:2208.01618*, 2022.
- Hertz, A., Mokady, R., Tenenbaum, J., Aberman, K., Pritch, Y., and Cohen-Or, D. Prompt-to-prompt image editing with cross-attention control. In *ICLR*, 2023.
- Heusel, M., Ramsauer, H., Unterthiner, T., Nessler, B., and Hochreiter, S. GANs trained by a two time-scale update rule converge to a local Nash equilibrium. *Advances in Neural Information Processing Systems (NIPS)*, 30, 2017.
- Hu, E. J., Shen, Y., Wallis, P., Allen-Zhu, Z., Li, Y., Wang, S., Wang, L., and Chen, W. Lora: Low-rank adaptation of large language models. *arXiv preprint arXiv:2106.09685*, 2021.
- Huang, Y., Xie, L., Wang, X., Yuan, Z., Cun, X., Ge, Y., Zhou, J., Dong, C., Huang, R., Zhang, R., et al. Smartedit: Exploring complex instruction-based image editing with multimodal large language models. In *Proceedings of the IEEE/CVF Conference on Computer Vision and Pattern Recognition*, pp. 8362–8371, 2024.
- Ju, X., Liu, X., Wang, X., Bian, Y., Shan, Y., and Xu, Q. Brushnet: A plug-and-play image inpainting model with decomposed dual-branch diffusion. In *European Conference on Computer Vision*, pp. 150–168. Springer, 2024.
- Kingma, D. P. Auto-encoding variational bayes. *arXiv preprint arXiv:1312.6114*, 2013.
- Kingma, D. P. and Ba, J. Adam: A method for stochastic optimization. *arXiv preprint arXiv:1412.6980*, 2014.
- Kirillov, A., Mintun, E., Ravi, N., Mao, H., Rolland, C., Gustafson, L., Xiao, T., Whitehead, S., Berg, A. C., Lo, W.-Y., et al. Segment anything. In *Proceedings of the IEEE/CVF International Conference on Computer Vision (ICCV)*, October 2023.
- Kumari, N., Zhang, B., Zhang, R., Shechtman, E., and Zhu, J.-Y. Multi-concept customization of text-to-image diffusion. In *Proceedings of the IEEE/CVF Conference on Computer Vision and Pattern Recognition*, pp. 1931–1941, 2023.
- Labs, B. F. Flux. <https://github.com/black-forest-labs/flux>, 2023.
- Li, D., Li, J., and Hoi, S. Blip-diffusion: Pre-trained subject representation for controllable text-to-image generation and editing. *Advances in Neural Information Processing Systems*, 36, 2024a.
- Li, Y., Liu, H., Wu, Q., Mu, F., Yang, J., Gao, J., Li, C., and Lee, Y. J. Gligen: Open-set grounded text-to-image generation. In *Proceedings of the IEEE/CVF Conference on Computer Vision and Pattern Recognition*, pp. 22511–22521, 2023.
- Li, Y., Bian, Y., Ju, X., Zhang, Z., Shan, Y., Zou, Y., and Xu, Q. Brushedit: All-in-one image inpainting and editing. *arXiv preprint arXiv:2412.10316*, 2024b.
- Lin, T.-Y., Maire, M., Belongie, S., Hays, J., Perona, P., Ramanan, D., Dollár, P., and Zitnick, C. L. Microsoft coco: Common objects in context. In *Computer Vision—ECCV 2014: 13th European Conference, Zurich, Switzerland, September 6–12, 2014, Proceedings, Part V 13*, pp. 740–755. Springer, 2014.
- Mahalanobis, P. On the generalized distance in statistics. National Institute of Science of India, 1936.
- Mu, J., Gharbi, M., Zhang, R., Shechtman, E., Vasconcelos, N., Wang, X., and Park, T. Editable image elements for controllable synthesis. In *European Conference on Computer Vision*, pp. 39–56. Springer, 2025.
- Nie, W., Liu, S., Mardani, M., Liu, C., Eckart, B., and Vahdat, A. Compositional text-to-image generation with dense blob representations. In *Forty-first International Conference on Machine Learning*, 2024.

- Nitzberg, M. and Mumford, D. B. *The 2.1-D sketch*. IEEE Computer Society Press, 1990.
- Oquab, M., Darcet, T., Moutakanni, T., Vo, H. V., Szafraniec, M., Khalidov, V., Fernandez, P., Haziza, D., Massa, F., El-Nouby, A., Howes, R., Huang, P.-Y., Xu, H., Sharma, V., Li, S.-W., Galuba, W., Rabbat, M., Assran, M., Ballas, N., Synnaeve, G., Misra, I., Jegou, H., Mairal, J., Labatut, P., Joulin, A., and Bojanowski, P. Dinov2: Learning robust visual features without supervision, 2023.
- Parmar, G., Patashnik, O., Wang, K.-C., Ostashev, D., Narasimhan, S., Zhu, J.-Y., Cohen-Or, D., and Aberman, K. Object-level visual prompts for compositional image generation. *arXiv preprint arXiv:2501.01424*, 2025.
- Porter, T. and Duff, T. Compositing digital images. In *Proceedings of the 11th annual conference on Computer graphics and interactive techniques*, pp. 253–259, 1984.
- Radford, A., Kim, J. W., Hallacy, C., Ramesh, A., Goh, G., Agarwal, S., Sastry, G., Askell, A., Mishkin, P., Clark, J., et al. Learning transferable visual models from natural language supervision. In *International conference on machine learning*, pp. 8748–8763. PMLR, 2021.
- Ramesh, A., Dhariwal, P., Nichol, A., Chu, C., and Chen, M. Hierarchical text-conditional image generation with clip latents. *arXiv preprint arXiv:2204.06125*, 1(2):3, 2022.
- Rombach, R., Blattmann, A., Lorenz, D., Esser, P., and Ommer, B. High-resolution image synthesis with latent diffusion models. In *CVPR*, 2022.
- Ruiz, N., Li, Y., Jampani, V., Pritch, Y., Rubinstein, M., and Aberman, K. Dreambooth: Fine tuning text-to-image diffusion models for subject-driven generation. In *Proceedings of the IEEE/CVF conference on computer vision and pattern recognition*, pp. 22500–22510, 2023.
- Serif Europe Ltd. Affinity photo, 2015–2023. URL <https://affinity.serif.com/photo/>. Version 2.0.
- Sheynin, S., Polyak, A., Singer, U., Kirstain, Y., Zohar, A., Ashual, O., Parikh, D., and Taigman, Y. Emu edit: Precise image editing via recognition and generation tasks. In *Proceedings of the IEEE/CVF Conference on Computer Vision and Pattern Recognition*, pp. 8871–8879, 2024.
- Shi, Y., Xue, C., Pan, J., Zhang, W., Tan, V. Y., and Bai, S. Dragdiffusion: Harnessing diffusion models for interactive point-based image editing. *arXiv preprint arXiv:2306.14435*, 2023.
- Shi, Y., Wang, P., and Huang, W. Seedit: Align image re-generation to image editing. *arXiv preprint arXiv:2411.06686*, 2024.
- Wang, Z., Bovik, A. C., Sheikh, H. R., and Simoncelli, E. P. Image quality assessment: from error visibility to structural similarity. *IEEE transactions on image processing*, 13(4):600–612, 2004.
- Wei, Y., Zhang, Y., Ji, Z., Bai, J., Zhang, L., and Zuo, W. Elite: Encoding visual concepts into textual embeddings for customized text-to-image generation. In *Proceedings of the IEEE/CVF International Conference on Computer Vision*, pp. 15943–15953, 2023.
- Wikipedia contributors. Peak signal-to-noise ratio — Wikipedia, the free encyclopedia, 2024. URL https://en.wikipedia.org/w/index.php?title=Peak_signal-to-noise_ratio&oldid=1210897995. [Online; accessed 4-March-2024].
- Xiong, Z., Xiong, W., Shi, J., Zhang, H., Song, Y., and Jacobs, N. Groundingbooth: Grounding text-to-image customization. *arXiv preprint arXiv:2409.08520*, 2024.
- Yang, B., Gu, S., Zhang, B., Zhang, T., Chen, X., Sun, X., Chen, D., and Wen, F. Paint by example: Exemplar-based image editing with diffusion models. In *Proceedings of the IEEE/CVF Conference on Computer Vision and Pattern Recognition*, pp. 18381–18391, 2023.
- Ye, H., Zhang, J., Liu, S., Han, X., and Yang, W. Ip-adapter: Text compatible image prompt adapter for text-to-image diffusion models. *arXiv preprint arXiv:2308.06721*, 2023.
- Zhang, H., Hong, D., Gao, T., Wang, Y., Shao, J., Wu, X., Wu, Z., and Jiang, Y.-G. Creatilayout: Siamese multi-modal diffusion transformer for creative layout-to-image generation. *arXiv preprint arXiv:2412.03859*, 2024a.
- Zhang, L., Rao, A., and Agrawala, M. Adding conditional control to text-to-image diffusion models, 2023a.
- Zhang, R., Isola, P., Efros, A. A., Shechtman, E., and Wang, O. The unreasonable effectiveness of deep features as a perceptual metric. In *Proceedings of the IEEE/CVF Conference on Computer Vision and Pattern Recognition (CVPR)*, pp. 586–595, 2018.
- Zhang, Y., Song, Y., Liu, J., Wang, R., Yu, J., Tang, H., Li, H., Tang, X., Hu, Y., Pan, H., et al. Ssr-encoder: Encoding selective subject representation for subject-driven generation. In *Proceedings of the IEEE/CVF Conference on Computer Vision and Pattern Recognition*, pp. 8069–8078, 2024b.
- Zhang, Z., Huang, Z., and Liao, J. Continuous layout editing of single images with diffusion models. In *Computer Graphics Forum*, pp. e14966. Wiley Online Library, 2023b.

A. BlobBench Overview and Evaluation Metrics

BlobBench Overview As shown in Figure 7, BlobBench is a comprehensive benchmark containing 100 curated images evenly distributed across different element-level operations (composition, movement, resizing, removal, and replacement). Each image is annotated with ellipse parameters, foreground masks, and text descriptions. The benchmark includes both real-world and AI-generated images across diverse scenarios like indoor/outdoor scenes, animals, and landscapes.

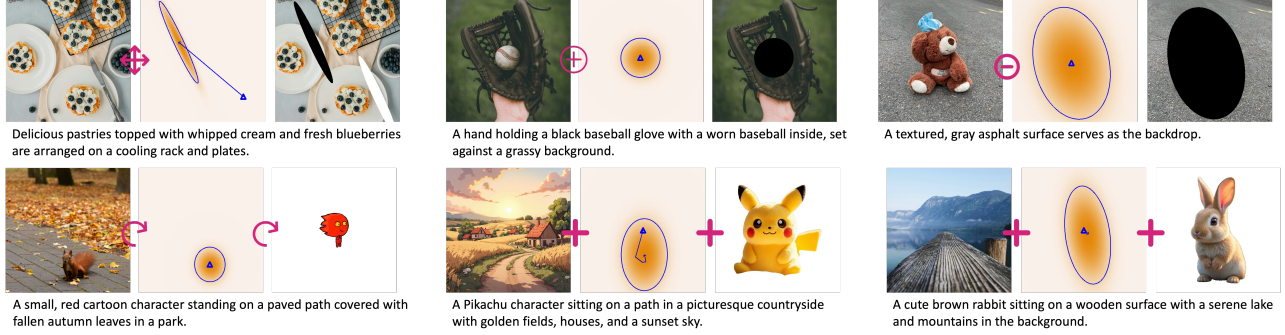


Figure 7: Overview of the BlobBench.

Evaluation Metrics For *objective evaluation*, we consider the following aspects:

- **Identity Preservation.** To evaluate element-level appearance preservation, we employ CLIP-I (Radford et al., 2021) and DINO (Caron et al., 2021) scores to measure the appearance similarity between generated and reference images.
- **Grounding Accuracy.** To evaluate layout control capability, we first extract masks from generated images using SAM (Kirillov et al., 2023) and fit ellipses or bounding box to these masks. We then compute the Mean Squared Error (MSE) between these fitted grounding annotations and the ground truth to quantify the accuracy of spatial control.
- **Generation Quality and Harmonization.** We adopt standard image quality metrics including FID (Heusel et al., 2017) for distribution similarity, PSNR (Wikipedia contributors, 2024) and SSIM (Wang et al., 2004) for pixel-level fidelity, and LPIPS (Zhang et al., 2018) for perceptual quality to evaluate both generation and editing results.

For *subjective evaluation*, we conduct a human study with 30 participants rating 20 sets of generated images on three aspects: fidelity, layout accuracy, and visual harmony. Each aspect is scored on a scale of 1-5, with 5 being the highest quality.

B. Mathematical Relationship Between Ellipses and 2D Gaussian Distributions

A 2D Gaussian distribution and an ellipse can be mathematically related through their covariance matrix and level sets. Here we explain their conversion:

From Gaussian to Ellipse. A 2D Gaussian distribution is formulated by its mean $\mu = (\mu_x, \mu_y)$ and covariance matrix Σ :

$$\Sigma = \begin{bmatrix} \sigma_x^2 & \rho\sigma_x\sigma_y \\ \rho\sigma_x\sigma_y & \sigma_y^2 \end{bmatrix} \quad (14)$$

The level sets of this distribution form ellipses. For a given confidence level α , the corresponding ellipse equation is:

$$(\mathbf{x} - \mu)^T \Sigma^{-1} (\mathbf{x} - \mu) = \chi_2^2(\alpha) \quad (15)$$

where $\chi_2^2(\alpha)$ is the quantile function for chi-square distribution with 2 degrees of freedom.

From Ellipse to Gaussian. Conversely, given an ellipse defined by its center (h, k) , semi-major axis a , semi-minor axis b , and rotation angle θ , we can construct the corresponding Gaussian distribution:

$$\mu = \begin{pmatrix} h \\ k \end{pmatrix} \quad (16)$$

$$\Sigma = \mathbf{R}(\theta) \begin{bmatrix} a^2 & 0 \\ 0 & b^2 \end{bmatrix} \mathbf{R}(\theta)^T \quad (17)$$

where $\mathbf{R}(\theta)$ is the 2D rotation matrix:

$$\mathbf{R}(\theta) = \begin{bmatrix} \cos \theta & -\sin \theta \\ \sin \theta & \cos \theta \end{bmatrix} \quad (18)$$

This mathematical relationship enables us to seamlessly transition between probabilistic blob representations and geometric ellipse controls in our framework.

C. BlobData Curation

BlobData is a large-scale dataset containing 1.86M samples sourced from BrushData (Ju et al., 2024), featuring images, segmentation masks, fitted ellipse parameters with derived 2D Gaussians, and descriptive texts. As shown in Fig. 8, the BlobData curation process involves multiple steps:

- **Image Filtering.** We filter source images to: 1) Retain images with shorter sides exceeding 480 pixels; 2) Keep only images with valid instance segmentation masks; 3) Apply mask filtering to preserve masks with area ratios between 0.01-0.9 of total image area; 4) Exclude masks touching image boundaries.
- **Parameter Extraction.** 1) Fit ellipse parameters using OpenCV’s ellipse fitting algorithm; 2) Derive corresponding 2D Gaussian distributions; 3) Remove invalid samples with covariance values below $1e-5$.
- **Annotation.** We generate detailed image descriptions using InternVL-2.5, providing rich textual context for each sample in the dataset.

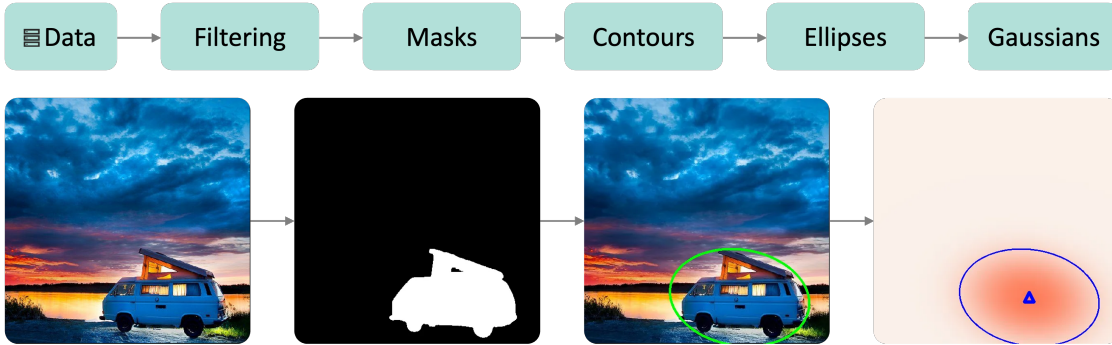


Figure 8: The BlobData curation workflow.